Efficient generation of hyperentangled photon pairs with controllable waveforms from cold atoms

Hui Yan[1,3] and Shi-liang Zhu[1,2,4]

[1]*Laboratory of Quantum Information Technology, School of Physics and Telecommunication Engineering, South China Normal University, Guangzhou 510006, China*
[2]*Center for Quantum Information, IIIS, Tsinghua University, Beijing 100084, China*
[3]*e-mail: yanhui@scnu.edu.cn*
[4]*e-mail: slzhu@scnu.edu.cn*

Received October 8, 2012; revised December 5, 2012; accepted December 14, 2012; posted December 19, 2012 (Doc. ID 177637); published January 16, 2013

We propose a scheme to efficiently generate time-frequency and polarization-entangled photon pairs with cold atomic ensembles via spontaneous four-wave mixing through combining the photon pairs from two symmetrical spatial modes by polarization beam splitters. With a two-dimensional magneto-optical trap, polarization-entangled photon pairs with controllable temporal length (>100 ns) can be generated at the rate of about 10^5 per second after taking into account all losses. Therefore, it is a feasible photon source for scalable linear optical quantum computation and long-distance quantum communication.

OCIS codes: 270.0270, 270.5585, 190.4410, 190.4380.

1. INTRODUCTION

Scalable linear optical quantum computation (LOQC) and quantum memory based long-distance quantum communication (LDQC) has attracted a great deal of interest recently [1–4]. For moving on, a feasible photonic entanglement source plays a critical role in those schemes [4]. For many decades, spontaneous parametric down-conversion in nonlinear crystals has been a standard method to generate nonclassical correlated photons [5]. However, such a source typically has a wide bandwidth (~THz) and short coherence time (~ps), and thus it is not suitable for LOQC and LDQC [3,6]. By putting the nonlinear crystal inside a cavity, generation of narrowband polarization-entangled photon pairs has been demonstrated [6,7].

Following the protocol of DLCZ proposed by Duan *et al.* [3], polarization-entangled photon pairs have been generated from atomic ensembles using a "writing-reading" technique [8–10]. For the spontaneous Raman transitions, the paired photons are generated in order. And hence, the paired photons are not time–frequency entangled. Subsequently, narrow bandwidth photon pairs have also been generated through electromagnetically induced transparency (EIT) and spontaneous four-wave mixing (SFWM) [11–13]. Recently, polarization entanglement has also been demonstrated experimentally using this technique [14]. However, due to the low efficiency of the right-angle geometry EIT, both the coherence time and generation rate are limited to less than 100 ns and several pairs per second, respectively [14]. Therefore, the generation of narrowband (MHz) polarization-entangled photon pairs with much higher generating rate is still in high demand.

In this paper, we propose a highly efficient scheme to generate hyperentangled (time-frequency and polarization-entangled) photon pairs through SFWM from cold atomic ensembles with controllable waveforms. It was proposed that the polarization-entangled photon pairs can be generated by using two SFWM channels in the atomic energy levels via right-angle geometry SFWM [15]. However, it was demonstrated that the generation rate is about several pairs per second due to the limitation of the right-angle configuration of SFWM [14]. Here, we propose to achieve polarization entanglement through combining the photon pairs from two symmetrical spatial modes of the SFWM by polarization beam splitters (PBS) instead of two FWM channels of the energy levels used in [14,15]. In addition, we calculate the generation rates as a function of the angle between the two symmetrical spatial modes. We find that the generation rate is lower when the angle is big, which is similar to that in [14,15]. In contrast, the generation rate can be five orders of magnitude larger when the angle is small. With this scheme, we show that narrowband hyperentangled photon pairs with controllable temporal length (100 ns to 1 μs) can be generated at the rate of about 10^5 s^{-1} after taking into account all of the losses. Those entangled photon pairs, with tunable optical frequencies near atomic resonances, are ideal for interacting and storing with atomic quantum memories [3,8,16–18], and hence may find many applications in LOQC and LDQC.

2. PROPOSED EXPERIMENTAL SETUP

The proposed scheme is shown in Fig. 1(a): counter-propagating pump laser with polarization σ^- and coupling laser with polarization σ^+ are collinear and set at the longitudinal axis of a two-dimensional (2D) magneto-optical trap (MOT) [19]; two Stokes (denoted as $s.L$, $s.R$) and two anti-Stokes (denoted by $as.L$, $as.R$) fields are collected at the angles $\pm\theta$ to the propagating direction of the pump and coupling beams, respectively. As shown in Fig. 1(b), for either one of the two space modes, only one four wave mixing (FWM) process can be picked up by the quarter wave plates (QWP) and PBS, i.e., for $s.L$ and $as.L$ fields, only the (σ^-, σ^-, σ^+, σ^+) process is picked up. Hence, the polarizations of the $s.L$ and $as.L$ fields should be σ^- and σ^+, respectively. After the QWP, the polarizations of both $s.L$ and $as.L$ fields are turned

0740-3224/13/020362-04$15.00/0

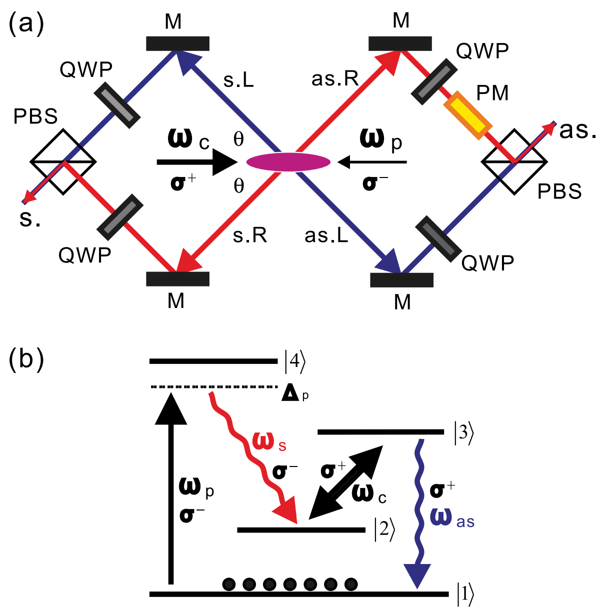

Fig. 1. (Color online) (a) Experimental setup. PBS: polarization beam splitter; M: mirror; QWP: quarter wave plate; PM: phase modulator. (b) Energy level configuration. ω_p: pump laser; ω_c: coupling laser; ω_s: Stokes field; ω_{as}: anti-Stokes field; Δ_p: pump laser detuning. As for ^{85}Rb, the energy levels $|1\rangle \to |4\rangle$ should be $|5S_{1/2}, F=2\rangle$, $|5S_{1/2}, F=3\rangle$, $|5P_{1/2}, F=3\rangle$, $|5P_{3/2}, F=3\rangle$, respectively.

to horizontal $|H\rangle$ and then collected by the PBS. On the other hand, the polarizations of both the $s.R(\sigma^-)$ and $as.R(\sigma^+)$ fields are turned into vertical $|V\rangle$ by the QWP. Photon pairs from other FWM processes are cleaned out by the two PBS. In the low-gain limit, the two symmetrical space modes of the Stokes and anti-Stokes fields have the same probability to generate one pair of photons. Thus, the paired photons are in a coherent superposition state before the PBS, i.e., $1/\sqrt{2}(|H_{s.L}H_{as.L}\rangle + |V_{s.R}V_{as.R}\rangle)$ (as mentioned above, σ^+ and σ^- photons are converted into horizontal $|H\rangle$ or vertical $|V\rangle$ polarized photons through $\lambda/4$ wave plates and then selected by PBS). Furthermore, after the PBS, the L/R road information is erased [9,10,20], so the photon pairs are entangled in polarization and the wave packet of the photon pairs is given by

$$|\Psi_{s,as}(t_s, t_{as})\rangle = \Psi(t_s, t_{as}) \frac{1}{\sqrt{2}} (|H_s H_{as}\rangle + e^{i\phi}|V_s V_{as}\rangle), \quad (1)$$

where t_s and t_{as} are the time of detecting a Stokes or an anti-Stokes photon, respectively, and ϕ is the entire phase difference between the two space modes before they overlap at PBS, which can be compensated and stabilized to 0 by the phase modulator (PM) as shown in Fig. 1 [21]. So the photon pairs can be kept in the maximally polarization-entangled state.

3. GENERATION RATE

Now we focus on one of the space modes before the PBS, such as the fields $s.L$ and $as.L$. It is a typical setup for generation of time-energy entangled narrowband photon pairs with cold atomic ensembles via EIT and backward geometry SFWM (with continuous pump and coupling lasers, Stokes and anti-Stokes photons are spontaneously generated and propagate in opposite directions) [11,12]. The four-level double-Λ atomic system is shown in Fig. 1(b). In the presence of a continuous-wave (cw) pump laser (ω_p) and a cw coupling (ω_c) laser, phase-matched Stokes (ω_s) and anti-Stokes (ω_{as}) photon pairs can be spontaneously produced from the FWM process in the low gain limit. As shown in Fig. 1(b), the resonant coupling laser forms a standard three-level Λ EIT system with the generated anti-Stokes field. So the coupling laser not only assists the FWM nonlinear process, but also creates a transparent window for the anti-Stokes photons with slow light effect. If we denote L as the length of the atomic ensemble, $V_g = |\Omega_c|^2/(2\rho\gamma_{13})$ (with $1/\gamma_{13}$ being the average lifetime of states $|1\rangle$ and $|3\rangle$) as the group velocity, then the coherence time ($\tau \approx L/V_g$) and the linewidth ($\Delta \approx 0.88/\tau$) of the photon pairs are determined by the coupling laser Ω_c and the optical density (OD) ρ of the cold atoms at the group delay region ($\tau > 1/\Omega_c, 1/\gamma_{13}$). With the perturbation theory [22], the wave packet of the photon pairs can be described as

$$\Psi(t_s, t_{as}) = \frac{L}{2\pi} \int \mathrm{d}\omega_{as} \kappa(\omega_{as}) \mathrm{sinc}\left(\frac{\Delta k L}{2}\right) \times e^{i(k_{as}+k_s)L/2} e^{-i\omega_{as}\tau} e^{-i(\omega_c+\omega_p)t_s}, \quad (2)$$

where $\tau = t_{as} - t_s$ and the phase mismatching $\Delta k = (k_{as} - k_s) + (k_p - k_c)\cos(\theta)$; k_{as} (k_s) stands for the wavenumber of anti-Stokes (Stokes) photons; k_p (k_c) stands for the wavenumber of pump (coupling) laser. The nonlinear parametric coupling coefficient $\kappa(\omega_{as}) = -i(\sqrt{\bar{\omega}_{as}\bar{\omega}_s}/2c)\chi^{(3)}(\omega_{as}, \omega_s)E_p E_c$, where $\chi^{(3)}$ is the third-order nonlinear susceptibility. $\bar{\omega}_{as}$ ($\bar{\omega}_s$) is the average frequency of the anti-Stokes (Stokes) photons, c is vacuum light speed, E_p (E_c) is the electric filed of the pump (coupling) laser. The photon pairs from the SFWM process should be time-energy entangled according to the wave function described in Eq. (2) [23].

The coincidence counts of the photon pairs can be determined by Glauber's theory with

$$G^{(2)}(t_s, t_{as}) = |\Psi(t_s, t_{as})|^2. \quad (3)$$

By using Eqs. (2) and (3), the coincidence counts can be calculated out. The results are plotted in Fig. 2(a) with different parameters at 1 ns time bin. The generation rate R is determined by the equation $R = \int G^{(2)}(t_s, t_{as})\mathrm{d}t$. When we choose the following typically experimental parameters $\rho = 40$, $\Omega_p = \gamma_{13}$, $\Omega_c = 4\gamma_{13}$, $\gamma_{13} = 2\pi \times 3$ MHz, $\Delta_p = -7.5\gamma_{13}$, $L = 1.5$ cm, $\theta = \pm 2°$, and also consider all the existence loss (fiber–fiber coupling efficiency 0.7, photon detector efficiency 0.5, filter efficiency 0.6), the generation rate is about 10^5 s^{-1}. As shown in Fig. 2(a), the coherence time or the linewidth is determined by ρ and Ω_c, while the generation rate is determined by ρ and Ω_p. In order to distinguish the photon pairs in time (this is also the low gain limit), the maximum generation rate we could obtain is limited by $\eta * 1/\tau$ (here $\eta \approx 0.1$ includes all the existence loss). For example, when $\tau = 500$ ns, the maximum generation rate we may obtain is about 2×10^5 s^{-1}. In order to suppress double-pair events, the generation rate should be set 1 or 2 magnitudes smaller. For comparison, the coincidence count for the right-angle FWM scheme is also plotted in Fig. 2(b) (here, the same parameters are selected as the above-proposed scheme; only

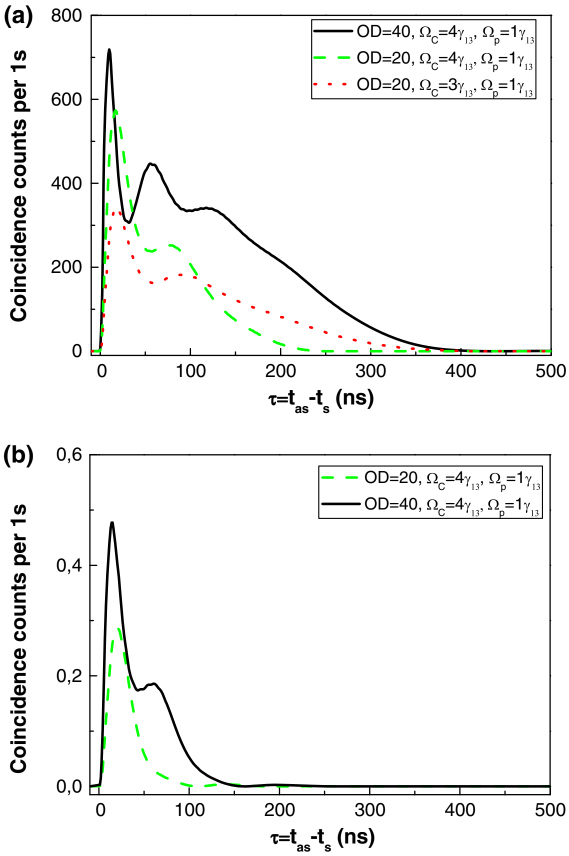

Fig. 2. (Color online) (a) Coincidence counts per second for the proposed scheme; generation rate and coincidence time are: 10^5 s^{-1} and 400 ns with (OD)$\rho = 40$, $\Omega_c = 4\gamma_{13}$ (solid curve); 0.5×10^5 s^{-1} and 200 ns with (OD) $\rho = 20$, $\Omega_c = 4\gamma_{13}$ (dotted curve), 0.5×10^5 s^{-1} and 360 ns with (OD) $\rho = 20$, $\Omega_c = 3\gamma_{13}$ (dashed curve). Other parameters: $\Omega_p = \gamma_{13}$, $\gamma_{13} = 2\pi \times 3$ MHz, $\Delta_p = -7.5\gamma_{13}$, $L = 1.5$ cm, $\theta = \pm 2°$, $\eta \approx 0.1$. (b) Coincidence counts per second for the right-angle FWM scheme (the same parameters are used as above; only $\Delta_p = 1000\gamma_{13}$ is different). With (OD) $\rho = 40$ (solid curve) and (OD) $\rho = 20$ (dashed line), only several pairs can be generated per second.

$\Delta_p = 1000\gamma_{13}$ is different that is limited by the scheme itself). Considering the absorption, the generating rate is only several pairs per second, which fits very well with the existing experiment [14,15].

4. POLARIZATION ENTANGLEMENT

In order to maintain the maximally polarization-entangled state, two symmetrical Stokes/anti-Stokes fields must be chosen in our scheme. For the phase-matching condition $[\Delta k = (k_{as} - k_s) + (k_p - k_c)\cos(\theta)]$, the generation rate is decreasing rapidly as θ increases, as shown in Fig. 3 (here we choose $\rho = 40$, $\Omega_p = \gamma_{13}$, $\Omega_c = 4\gamma_{13}$, $\gamma_{13} = 2\pi \times 3$ MHz, $\Delta_p = -7.5\gamma_{13}$, $L = 1.5$ cm, $\eta \approx 0.1$). When $\theta \to 90°$, only several pairs of photons per second could be generated. This is the same as the right-angle geometry SFWM [14,15]. In those schemes, in order to obtain two undistinguished FWM channels, the energy levels of right-angle geometry SFWM must be chosen. Thus the efficiency couldn't be kept high. In addition, for the right-angle FWM, the absorption is another important reason for the low efficiency because the right-angle EIT couldn't get 100% transparency besides the phase mismatch.

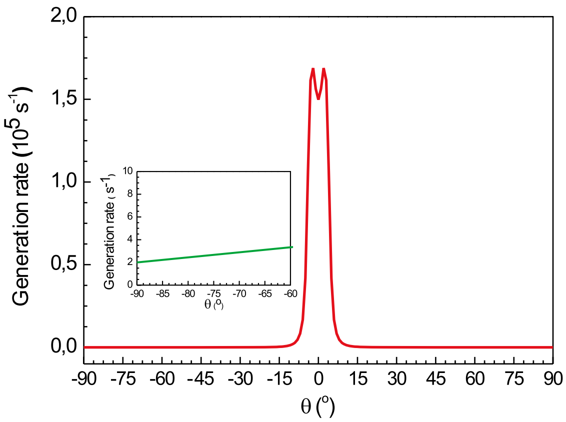

Fig. 3. (Color online) Generation rate versus θ; the insert is the enlarged region around $\theta = 90°$. Other parameters: $\rho = 40$, $\Omega_p = \gamma_{13}$, $\Omega_c = 4\gamma_{13}$, $\gamma_{13} = 2\pi \times 3$ MHz, $\Delta_p = -7.5\gamma_{13}$, $L = 1.5$ cm, $\eta \approx 0.1$.

Compared with the right-angle scheme, a great advantage in the present scheme is that the angle θ can be varied between 0 to $\pi/2$ since only two symmetrical space modes are needed. As shown in Fig. 3, when $-10° < \theta < 10°$, the generation rate is almost the same; thus, it will be easy to choose two symmetrical Stokes/anti-Stokes fields in our setup. In addition, when $\theta \approx 5°$, we get the maximum generation rate for the best phase-matching condition.

Besides the generation rate, the visibility of the interference fringe of the polarization correlation between Stokes and anti-Stokes photons, which determines the degree of entanglement, is another crucial parameter for the proposed scheme. In the low gain limit, the visibility is given by [10]

$$V = \frac{g^{(2)}_{s,as} - 1}{g^{(2)}_{s,as} + 1}, \tag{4}$$

where the normalized cross-correlation function $g^{(2)}_{s,as} = 1 + G^{(2)}(t_s, t_{as})/(R_s R_{as})$ with R_s and R_{as} being the single-photon rates of Stokes and anti-Stokes photons [14,20], respectively. As shown in Fig. 4, the visibility V can be larger than $1/\sqrt{2}$ in the condition $g^{(2)}_{s,as} > 6$, while $V = 1/\sqrt{2}$ is

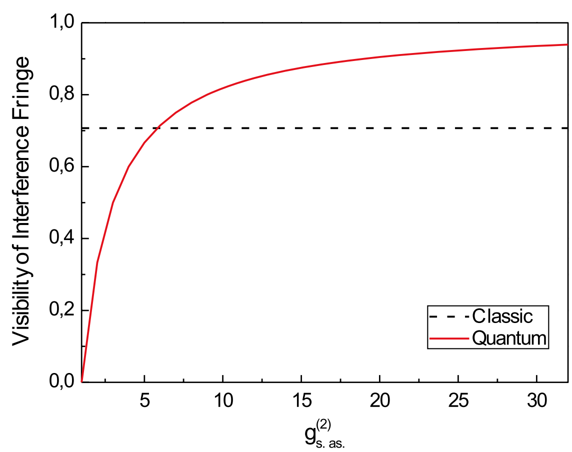

Fig. 4. (Color online) Visibility of the interference fringe of the polarization correlation between Stokes and anti-Stokes photons. The dashed line is the boundary of $1/\sqrt{2}$, which is the limit to violate the Bell–CHSH inequality, while the solid curve is the visibility V versus $g^{(2)}_{s,as}$.

actually the limit to violate the Bell–CHSH inequality and indicates the polarization entanglement [24]. Notably, the previous experiments had shown that it is easy to obtain $g^{(2)}_{s,as} > 10$ [11,12,25].

5. CONCLUSION

In summary, we have proposed a scheme to efficiently generate narrowband hyperentangled photon pairs with 2D MOT through SFWM. These narrowband hyperentangled photon pairs, with generation rate larger than 10^5 s^{-1} and coherence time longer than 100 ns, are suitable for LOQC and quantum memory-based LDQC. Comparing with the "writing-reading" scheme, our scheme is a continuous source, and the generated photons are also time-frequency entangled besides the polarization. In addition, the waveform can be adjustable for the slow light effect [14,25]. In addition, photons simultaneously entangled in more than one degree of freedom (such as polarization, momentum, and time-frequency), are useful in increasing information capacity in quantum communication [26,27].

ACKNOWLEDGMENTS

The authors acknowledge helpful discussions with S. W. Du. This work was supported by the NSF of China (Nos. 11104085, 10974059, 11125417), the Major Research Plan of the National Natural Science Foundation of China (No. 91121023), the NBRPC (No. 2011CBA00302), the SKPBR of China (No. 2011CB922104), and the PCSIRT.

REFERENCES

1. E. Knill, R. Laflamme, and G. J. Milburn, "A scheme for efficient quantum computation with linear optics," Nature **409**, 46–52 (2001).
2. D. Browne and T. Rudolph, "Resource-efficient linear optical quantum computation," Phys. Rev. Lett. **95**, 010501 (2005).
3. L. M. Duan, M. D. Lukin, M. D. Cirac, and P. Zoller, "Long-distance quantum communication with atomic ensembles and linear optics," Nature **414**, 413–418 (2001).
4. H. Zhang, X. Jin, J. Yang, H. Dai, S. Yang, T. Zhao, J. Rui, Y. He, X. Jiang, F. Yang, G. Pan, Z. Yuan, Y. Deng, Z. Chen, X. Bao, S. Chen, B. Zhao, and J. W. Pan, "Preparation and storage of frequency-uncorrelated entangled photons from cavity-enhanced spontaneous parametric downconversion," Nat. Photonics **5**, 628–632 (2011).
5. P. G. Kwiat, K. Mattle, H. Weinfurter, A. Zeilinger, A. V. Sergienko, and Y. Shih, "New high-intensity source of polarization-entangled photon pairs," Phys. Rev. Lett. **75**, 4337–4341 (1995).
6. X. H. Bao, Y. Qian, J. Yang, H. Zhang, Z. B. Chen, T. Yang, and J. W. Pan, "Generation of narrow-band polarization-entangled photon pairs for atomic quantum memories," Phys. Rev. Lett. **101**, 190501 (2008).
7. Z. Y. Ou and Y. J. Lu, "Cavity enhanced spontaneous parametric down-conversion for the prolongation of correlation time between conjugate photons," Phys. Rev. Lett. **83**, 2556–2559 (1999).
8. D. Matsukevich and A. Kuzmich, "Quantum state transfer between matter and light," Science **306**, 663–666 (2004).
9. J. Laurat, K. S. Choi, H. Deng, C. W. Chou, and H. J. Kimble, "Heralded entanglement between atomic ensembles: preparation, decoherence, and scaling," Phys. Rev. Lett. **99**, 180504 (2007).
10. S. Chen, Y.-A. Chen, B. Zhao, Z.-S. Yuan, J. Schmiedmayer, and J.-W. Pan, "Demonstration of a stable atom-photon entanglement source for quantum repeaters," Phys. Rev. Lett. **99**, 180505 (2007).
11. V. Balic, D. A. Braje, P. Kolchin, G. Y. Yin, and S. E. Harris, "Generation of paired photons with controllable waveforms," Phys. Rev. Lett. **94**, 183601 (2005).
12. S. W. Du, P. Kolchin, C. Belthangady, G. Y. Yin, and S. E. Harris, "Subnatural linewidth biphotons with controllable temporal length," Phys. Rev. Lett. **100**, 183603 (2008).
13. X. S. Lu, Q. F. Chen, B. S. Shi, and G. C. Guo, "Generation of a non-classical correlated photon pair via a spontaneous four-wave mixing in a cold atomic ensemble," Chin. Phys. Lett. **26**, 064204 (2009).
14. H. Yan, S. C. Zhang, J. F. Chen, M. M. T. Loy, G. K. L. Wong, and S. Du, "Generation of narrow-band hyperentangled nondegenerate paired photons," Phys. Rev. Lett. **106**, 033601 (2011).
15. S. Du, E. Oh, J. Wen, and M. H. Rubin, "Four-wave mixing in three-level systems: interference and entanglement," Phys. Rev. A **76**, 013803 (2007).
16. C. H. van der Wal, M. D. Eisaman, A. Andre, R. L. Walsworth, D. F. Phillips, A. S. Zibrov, and M. D. Lukin, "Atomic memory for correlated photon states," Science **301**, 196–200 (2003).
17. A. Kuzmich, W. P. Bowen, A. D. Boozer, A. Boca, C. W. Chou, L. M. Duan, and H. J. Kimble, "Generation of nonclassical photon pairs for scalable quantum communication with atomic ensembles," Nature **423**, 731–734 (2003).
18. F. Mei, Y. F. Yu, X. L. Feng, Z. M. Zhang, and C. H. Oh, "Quantum entanglement distribution with hybrid parity gate," Phys. Rev. A **82**, 052315 (2010).
19. Y. W. Lin, H. C. Chou, P. P. Dwivedi, Y. C. Chen, and I. A. Yu, "Using a pair of rectangular coils in the MOT for the production of cold atom clouds with large optical density," Opt. Express **16**, 3753–3761 (2008).
20. S. Chen, Y. A. Chen, T. Strassel, Z. S. Yuan, B. Zhao, J. Schmiedmayer, and J. W. Pan, "Deterministic and storable single-photon source based on a quantum memory," Phys. Rev. Lett. **97**, 173004 (2006).
21. Z. S. Yuan, Y. A. Chen, B. Zhao, S. Chen, J. Schmiedmayer, and J. W. Pan, "Experimental demonstration of a BDCZ quantum repeater," Nature **454**, 1098–1101 (2008).
22. S. W. Du, J. M. Wen, and M. H. Rubin, "Narrowband biphoton generation near atomic resonance," J. Opt. Soc. Am. B **25**, C98–C108 (2008).
23. J. D. Franson, "Bell inequality for position and time," Phys. Rev. Lett. **62**, 2205–2208 (1989).
24. J. F. Clauser, M. A. Horne, A. Shimony, and R. A. Holt, "Proposed experiment to test local hidden-variable theories," Phys. Rev. Lett. **23**, 880–884 (1969).
25. J. F. Chen, S. Zhang, H. Yan, M. M. T. Loy, G. K. L. Wong, and S. Du, "Shaping biphoton temporal waveforms with modulated classical fields," Phys. Rev. Lett. **104**, 183604 (2010).
26. C. Wang, F. G. Deng, Y. S. Li, X. S. Liu, and G. L. Long, "Quantum secure direct communication with high-dimension quantum superdense coding," Phys. Rev. A **71**, 044305 (2005).
27. H. Yan, S. L. Zhu, and S. W. Du, "Efficient phase-encoding quantum key generation with narrow-band single photons," Chin. Phys. Lett. **28**, 070307 (2011).